Preprints (www.preprints.org) | NOT PEER-REVIEWED | Posted: 13 November 2018 doi:10.20944/preprints201811.0302.v1

Peer-reviewed version available at *Energies* **2019**, *12*, 189; doi:10.3390/en12010189

Article

Medium-Term Hydropower Scheduling with Variable Head under Inflow, Energy and Reserve Capacity Price Uncertainty

Martin N. Hjelmeland[1,*], Arild Helseth[2], and Magnus Korpås[1]

[1] NTNU Norwegian University of Science and Technology, Trondheim, Norway
[2] SINTEF Energy Research, Trondheim, Norway
* Correspondence: martin.hjelmeland@ntnu.no

Abstract: We propose a model for medium-term hydropower scheduling (MTHS) with variable head and uncertainty in inflow, reserve capacity, and energy price. With an increase of intermittent energy sources in the generation mix, it is expected that a flexible hydropower producer can obtain added profits by participating in other markets than just the energy market. To capture this added potential the hydropower system should be modeled with a higher level of details. In this context, we apply an algorithm based on stochastic dual dynamic programming (SDDP) to solve the nonconvex MTHS problem, and show that the use of Strengthened Benders (SB) cuts to represent the expected future profit (EFP) function provide accurate scheduling results for slightly nonconvex problems. A method to visualize the EFP function in a dynamic programming setting is provided, serving as a useful tool for a priori inspection of the EFP shape and its nonconvexity.

Keywords: Hydropower scheduling; Stochastic programming; Integer programming

1. Introduction

Increasing rates of renewable energy generation are resulting in a higher demand for flexible power units to balance the power system and to deliver ramping capacity. Regulated hydropower is a flexible renewable energy source that is well suited to provide such services. The increased demand for flexibility has led to the requirement of more detailed optimization models, such that the flexible power units can perform an optimal allocation of resources in the different power markets for energy and ancillary services. In this work, we focus on rotating reserve capacity, providing what is normally referred to as primary and secondary reserves.

The Stochastic Dual Dynamic Programming (SDDP) algorithm proposed in [1] is commonly used for hydropower scheduling, and can be seen as a sampling-based approach of the nested Benders decomposition proposed in [2]. The sampling based method for solving multistage stochastic programming problems consists of two main procedures; the forward and backward pass. Instead of visiting all nodes in the scenario tree, the forward pass samples a set of scenarios used to generate candidate solutions. The backward pass follows the trajectories of the candidate solutions computed in the forward pass, starting from the final stage, to approximate the expected future profit (EFP) function. Subsequently, a statistical confidence interval can be computed for controlling the convergence of the method. A more in-depth explanation of the method can be found in [3–5].

In this work we investigate how improvements in the SDDP algorithm, derived from the Stochastic Dual Dynamic integer Programming (SDDiP) algorithm [6], can be used to improve the Medium-Term Hydropower Scheduling (MTHS) problem under uncertainty. The MTHS problem normally covers a planning horizon of one to three years, aiming at maximizing a single producer's expected profit. We

© 2018 by the author(s). Distributed under a Creative Commons CC BY license.

Preprints (www.preprints.org) | NOT PEER-REVIEWED | Posted: 13 November 2018 doi:10.20944/preprints201811.0302.v1

Peer-reviewed version available at Energies 2019, 12, 189; doi:10.3390/en12010189

have from ongoing research experienced that SDDiP requires considerable more computational force than SDDP [7]. Nevertheless, an improved type of the Benders (B) cuts, called Strengthened Benders (SB) cuts, derived from the SDDiP method, show promising results by improving convergence of the algorithm with an reasonable increase in computation time. The generation of SB cuts requires solving an additional Mixed Integer Programming (MIP) problem to compute the right-hand-side parameter of the cut. This provides an at least as good cut as the original B cut.

A considerable amount of research has been conducted for solving the nonconvex MTHS problem, such as [8–11]. Except from [10] that proposed an novel approach that uses step functions to model a nonconvex EFP function, they all rely on solving some relaxation of the original problem. This is also the case for the SB cuts applied in this work. However, instead of solving the Lagrangian problem to convergence to obtain the cuts, one solves the Lagrangian problem only once, as elaborated in Section 3.2.

For the MTHS problem, a hybrid Stochastic Dynamic Programming (SDP) - SDDP method is currently the state-of-the-art in the Nordic power system. This method was developed in the late 90s and uses a discrete Markov chain to describe the price uncertainty and an autoregressive model to describe the inflow to the reservoirs [5,12]. The discrete Markov chain is used to circumvent the nonconvexity caused by the bilinear term where the energy price and the generation are multiplied. As the uncertainty is described by two different stochastic processes, it is challenging to model correlations between these processes. For an MTHS problem with weekly decision stages, it has been shown that the correlation between inflow and energy price has not been too significant on a weekly basis, yielding sufficient results by the hybrid SDP/SDDP method [12]. Nonetheless, adding additional markets would extend the dimension of the Markov chain. This comes at a significant increase of computational cost, as presented in in [13], where a reserve capacity market was added to the Markov process for an MTHS problem. The recent works [14] and [15], propose an elegant approach for including uncertainty in the objective function for dynamic programming (DP) problems, utilizing the fact that the EFP function is a saddle function that is convex w.r.t. to the objective coefficient and concave w.r.t. the state variables. In the following work, we build on the work in [15] to model the MTHS problem with uncertain of inflow, energy, and reserve capacity price.

1.1. Contributions

The work carried out in this paper is based on earlier work on developing improved methods to solve the MTHS problem, as in [7,16]. The main contributions are:

- A procedure to visualize and evaluate the shape of the EFP function to give a better intuition of nonconvexities in dynamic programming problems.
- The application of SDDP with SB cuts on a realistic nonconvex MTHS case study. The SDDP model considers correlated stochastic processes of inflow, energy and reserve capacity price.
- The representation of nonconcave generation functions that are dependent on discharge and water head by concave regions.

2. The Medium-Term Hydropower Scheduling (MTHS) Problem

A dense formulation of the MTHS problem is given as the following multistage stochastic programming problem

$$\max_{(x_1,y_1),\dots,(x_T,y_T)} \mathbb{E}_{\tilde{\xi}}\left\{\sum_{t=1}^{T} f_t(x_t,y_t,\tilde{\xi}_t)\right\} \tag{1a}$$

Preprints (www.preprints.org) | NOT PEER-REVIEWED | Posted: 13 November 2018 doi:10.20944/preprints201811.0302.v1

Peer-reviewed version available at Energies 2019, 12, 189; doi:10.3390/en12010189

$$\text{s.t.} \quad Wx_t + Hx_{t-1} + Gy_t = h(\tilde{\xi}_t) \tag{1b}$$
$$By_t = 0 \tag{1c}$$
$$Cy_t - Dx_t \geq 0 \tag{1d}$$
$$Cy_t + Dx_t \leq Cy^{\max} \tag{1e}$$
$$(x_t, y_t) \in Y_t \tag{1f}$$
$$x_t \in \mathbb{R}^{k_1} \cdot \mathbb{Z}^{k_2}, y_t \in \mathbb{R}^{l_1} \cdot \mathbb{Z}^{l_2} \tag{1g}$$
$$\forall t \in \{1, 2, \ldots, T\}. \tag{1h}$$

The state variables, x_t, carry information between stages with a known initial state, x_0. Stage variables are given by y_t. The objective is to maximize the expected value of some real value function f_t, that describes the profit the system can obtain. The expectation is taken over $\tilde{\xi}_t$ that describes a stochastic processes of the inflow to the reservoirs as well as energy, and reserve capacity prices. The matrices W, H, G, B, C, D are of suitable dimensions and define the parameters for a given hydropower system. The time-linking constraints (1b), constrain the unit commitment of hydro stations and provide reservoir balances, where the function $h(\tilde{\xi}_t)$ describes the inflows to the reservoirs. The energy balance is given by (1c). The systems ability to provide reserve capacity is included in (1d) and (1e). The generation function defining the relationship between power output, discharge and net head for each station, and the head function, describing how head is related to reservoir volume, are also described by these constraints. More details on the these functions are given in Section 2.1. Other system constraints, not imperative for this study, are given in (1f).

In contrast to earlier characterizations of the MTHS problem, such as [5], where the objective was to maximize income from selling only energy, we extend this to include sales of reserve capacity. In order to keep the MTHS tractable, we define the reserve capacity as a composition of the provision of primary and secondary reserves. Further operational details associated with participation in the different markets are left for the Short-Term Hydropower Scheduling (STHS) problem [17] to handle.

2.1. Generation Function

The generation function describes a power stations power output. An illustration is given in Figure 1, where the generation is a function of discharge and net head. The station consists of two units, as can be seen from the two concave regions along the water discharge in Figure 1.

Due to the computational complexity of the MTHS problem, the generation function is normally cast as a concave function, where the power output only depends on discharge. For a well-regulated and loosely constrained hydropower system where the producer only considers sales of energy, this assumption is reasonable. Roughly speaking, the optimal solution is to discharge as much water as possible in the hours with the highest energy prices and produce nothing the rest of the year. But as discussed in Section 1 we expect that hydropower plants will more frequently run at low-level power output in the future to provide ancillary services. This behaviour might also be imposed by environmental constraints, such as minimum discharge limits certain periods throughout the year. While operating at low power outputs, the linear optimization model will observe a higher power output than what is physically feasible and thus overestimate the system's potential profit, as discussed in [7,16]. This overestimation can be avoided by more accurate modelling of the generation function. However, such improvements bring about increased model complexity and computation time. In the following, we define the generation function as a nonconcave function of net head and discharge. The generation function of a power station, for a given stage t is defined by the following

Preprints (www.preprints.org) | NOT PEER-REVIEWED | Posted: 13 November 2018 doi:10.20944/preprints201811.0302.v1

Peer-reviewed version available at Energies 2019, 12, 189; doi:10.3390/en12010189

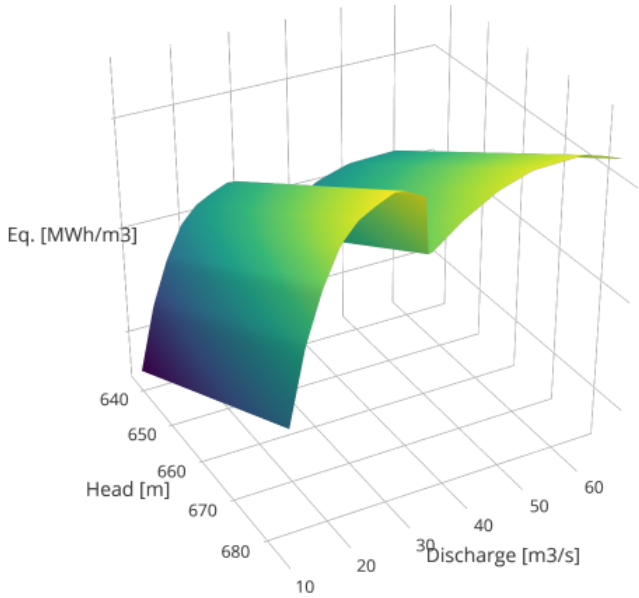

Figure 1. A generation function dependent on net head and discharge. For the purpose of illustration the z-axis is given by the energy equivalent ([MWh/m^3]).

$$p_c \leq \alpha_i q_c + b_i x_c + \beta_i h, \forall i \in \mathcal{K}(c), \forall c \in \mathcal{C} \tag{2a}$$
$$Q_c^{\min} x_c \leq q_c \leq Q_c^{\max} x_c, \forall c \in \mathcal{C} \tag{2b}$$
$$P_c^{\min} x_c \leq p_c \leq P_c^{\max} x_c, \forall c \in \mathcal{C} \tag{2c}$$
$$\sum_{c \in \mathcal{C}} x_c \leq 1 \tag{2d}$$
$$x_c \in \{0,1\}, (p_c, q_c) \in \mathbb{R}_+ \tag{2e}$$

Where h is the net head, i.e., height difference between the station's upstream reservoir and the tailwater level. The set $\mathcal{C}$ contains concave regions of the generation function, where the discharge, q_c, and generation, p_c, is constructed for each of these regions. For each concave region the generation function is bounded above by a set of hyperplanes, $\mathcal{K}(c)$, with coefficients $\alpha_{i(c)}$ and $\beta_{i(c)}$, and a right-hand side parameter $b_{i(c)}$. The generation function is describing the entire station's power output, therefore, one must make an assumption that the units are started in a certain sequence. These sequence of starting up new units leads to nonconcavities in the generation function, as seen in Figure 1. Also, another source of nonconcavity comes from the fact that power output for a hydropower station is a nonconcave function w.r.t. head. Therefore, one must make a trade-off between accurate problem formulation and computation time. To tackle this, we base our implementation of the generation function presented in [16].

Several authors have investigated how to include variable head in the hydropower scheduling problem. Most of the publications are related to solving the STHS problem, see [17–20]. There has also been some work conducted on how to include variable head in MTHS problems [8,21]. A nonconcave generation function is described in [8], using a piecewise-linear approximation. The formulation in [8] requires one binary variable for each discrete point of the generation function, compared to one binary variable for each concave region in (2). In [21] the generation function is approximated by hyperplanes, and the authors propose a quadratic function to describe the relationship between head and reservoir volume. The bilinear terms are divided into a grid with different cells, where each sell is represented by McCormick envelopes. Our approach avoids the bilinear term as the generation function is described by a set of hyperplanes for each of the concave regions. The method of using

Preprints (www.preprints.org) | NOT PEER-REVIEWED | Posted: 13 November 2018 doi:10.20944/preprints201811.0302.v1

Peer-reviewed version available at Energies 2019, 12, 189; doi:10.3390/en12010189

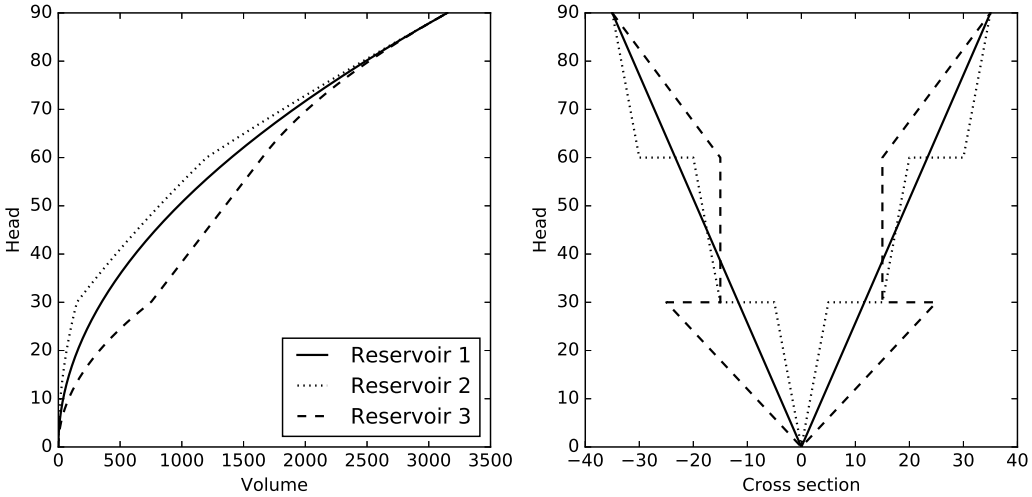

Figure 2. (Right) cross-section of some artificial hydropower reservoirs. (Left) head as a function of reservoir volume for the same reservoirs (corresponding line style). It is assumed that, from the view of the cross-section, the reservoirs has a depth of 1 unit.

hyperplanes to describe the generation function is not novel, e.g. proposed in [20], our approach is thus an extension to an already established methodology.

The head function, relating head and reservoir volume, can for most Norwegian reservoirs be approximated by a concave function without significantly comprising accuracy. An illustration of this is given in Figure 2, where the head function is illustrated with some constructed reservoirs. One can observe that the head function is concave for a reservoir with a monotonically increasing cross-section, but may be nonconcave for a reservoir that inhabits a subsurface cave.

2.2. Stochastic Processes

For solving the MTHS problem with uncertain, inflow, energy and reserve capacity price we apply a Vector Autoregressive Model of order 1 (VAR-1), see (3).

$$n_t = \Phi n_{t-1} + \tilde{\xi}_t \tag{3}$$

$$r_t = \mu_t + \sigma_t n_t. \tag{4}$$

Where n_t is the vector of the normalized stochastic processes, Φ is a time-invariant correlation matrix and $\tilde{\xi}_t$ is a vector of white noise with realizations denoted as ξ_t. The physical realizations r_t of the normalized variables are given by (4), where μ_t and σ_t are the expected value and standard deviation of the processes. p_t is defined as the subset of r_t that describes the objective term coefficients. As described in [15], these coefficients must be computed a priori to solving the stagewise decision problem. Thus, the energy and reserve capacity prices are found beforehand and provided as a parameters to the stagewise decision problem, while the constraints on the normalized inflows are included in the weekly decision problem. Note that the normalized inflows can be calculated a priori and provided to the optimization problem as a parameter, but for modelling convenience they are added as constraints. The treatment of objective term uncertainty in the SDDP method was first described in [15] and is further discussed in Section 3.3.

Preprints (www.preprints.org) | NOT PEER-REVIEWED | Posted: 13 November 2018 doi:10.20944/preprints201811.0302.v1

Peer-reviewed version available at Energies 2019, 12, 189; doi:10.3390/en12010189

3. Methodology

The following section first describes how one can visualize and inspect the EFP function. Followingly, it gives some insight how the uncertain objective function is included and how the SB cuts introduced in [6] are used to solve the MTHS problem with variable head and price uncertainty.

3.1. The EFP Visualization Approach

In order to get insight into the shape of EFP function we solve the extensive form of problem (1). By visually inspecting the EFP function one can get a first-hand impression whether it can be approximated using SB cuts with sufficient accuracy or not.

To solve the extensive problem of (1) we rely on a tractable scenario tree representing some of the underlying uncertainty with a one-year planning horizon. Then by looping over different initial reservoir levels, re-solving (1) and storing the objective value, one can obtain an estimate of the EFP function for the first stage. This procedure is performed for some cases of the MTHS problem with and without capacity reserves, as seen in Figure 3.

The approach is limited in the sense that it only provides an approximation of the EFP function for a given time stage. Moreover, it can only provide meaningful visualizations a few state variables at the time. The results should therefore only assist the modeller on what approach to use. Note that this visual approach can be combined with numerical indices, such as those presented in [22], for indicating the degree of nonconcavity of the MTHS problem.

3.1.1. Inspecting the EFP for the MTHS at hand

The MTHS problem (1) was defined with different head functions; a highly concave, highly nonconcave, constant and the actual function for a given reservoir. They are illustrated in the right plot in Figure 3. The resulting EFP function is given in the two leftmost plots, where the plot to the left included sales of reserve capacity. It is clear that the shape of the head function has a significant impact on the corresponding shape of the EFP function, yielding information that can be used for deciding which solution strategy, and possible required simplifications, one should use.

The two EFP functions corresponding to constant head are plotted (in black, stapled lines). One of them is the Linear Programming (LP) relaxation, noted as PQH^{LP}. As expected, the LP relaxation yield a concave EFP function. Moreover, the LP relaxation significantly overestimates the EFP function. Since the EFP function with the actual head function is not a highly nonconcave function, we expect that representing the generation function by piecewise-linear functions (cuts) provides acceptable results.

3.2. DP Formualtion

In SDDP the forward pass is used to generate valid candidate solutions that are used for computing the EFP function in the backward pass. All possible candidate solutions generated in the forward pass must, therefore, be present in the solution space in the problem used in the backward pass. The EFP function is described by an upper approximated piecewise-linear concave function, generated in the backward pass. For the forward pass, we define the following DP problem for iteration i

$$\text{FP}_t^i: \; Q_t^i(x_{t-1}, u_{t-1}, \xi_t) := \max_{x_t, y_t, z_t, u_t} f_t(x_t, y_t, u_t, \xi_t) + \phi_t^i(x_t, u_t, \tilde{\xi}_{t+1}) \tag{5a}$$

$$\text{s.t.} \quad (z_t, x_t, y_t) \in X_t(\xi_t) \tag{5b}$$

$$z_t = x_{t-1} \tag{5c}$$

$$(z_t, u_t) \in \mathbb{R}, (x_t, y_t) \in \mathbb{R} \cdot \mathbb{Z}. \tag{5d}$$

The objective function (5a) consist of the present profit function, f_t, and the EFP function ϕ_t^i. The problem is constrained by the set X_t and the copy constraint (5c) as described in [6] together with the

Preprints (www.preprints.org) | NOT PEER-REVIEWED | Posted: 13 November 2018 doi:10.20944/preprints201811.0302.v1

Peer-reviewed version available at Energies 2019, 12, 189; doi:10.3390/en12010189

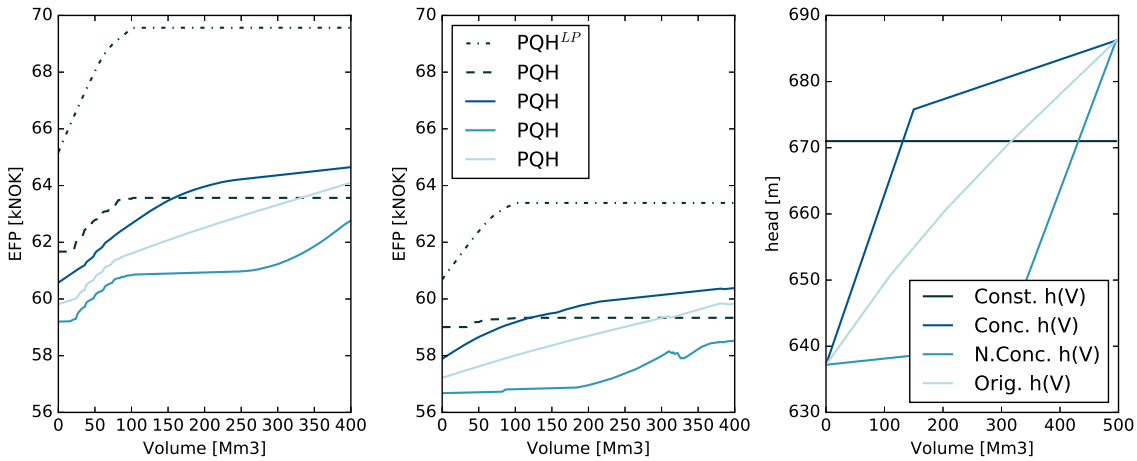

Figure 3. (Left) EFP with sales of reserve capacity and energy. (Middle) EFP with sales of energy. (Right) different head functions. The colors of the lines in the two leftmost figures refer to the head function, $h(V)$, in the right figure. The PQH^{LP} function refers to the LP relaxation of (1). Both stapled lines refer to the constant water head, thus the power output only depends on discharge.

copy variable z_t. In addition to the state and stage variables (x_t and y_t) the additional state variable u_t is included in the formulation to include the uncertain objective coefficients, as discussed in [15].

In order to compute the EFP function, we define a backward pass problem, BP_t^i, where integrality has been relaxed.

$$\mathrm{BP}_t^i: \ \mathcal{Q}_t^i(x_{t-1}, u_{t-1}, \xi_t) := \max_{x_t, y_t, z_t, u_t} f_t(x_t, y_t, u_t, \xi_t) + \phi_t^i(x_t, u_t, \tilde{\xi}_{t+1}) \tag{6a}$$

$$\text{s.t.} \quad (z_t, x_t, y_t) \in X_t(\xi_t) \tag{6b}$$

$$z_t = x_{t-1} \tag{6c}$$

$$(z_t, u_t, x_t, y_t) \in \mathbb{R}. \tag{6d}$$

By solving BP_t^i we obtain the cut coefficients π_t^i, from the dual values of the copy constraint in (6c). The cut coefficients aligned with the objective-term uncertainty is purely given by the sampled value, as described in [15]. Further, the cut used to describe the EFP function is enhanced by solving the following Lagrangian problem,

$$\mathrm{LG}_t^i: \ \mathcal{L}_t^i(\pi_t) := \max_{x_t, y_t, z_t, u_t} f_t(x_t, y_t, u_t, \xi_t) + \phi_t^i(x_t, u_t, \tilde{\xi}_{t+1}) - \pi_t^\top z_t \tag{7a}$$

$$\text{s.t.} \quad (z_t, x_t, y_t) \in X_t(\xi_t) \tag{7b}$$

$$(z_t, u_t) \in \mathbb{R}, (x_t, y_t) \in \mathbb{R} \cdot \mathbb{Z}, \tag{7c}$$

based on a Lagrangian relaxation of problem FP_t^i. By solving the Lagrangian problem one can obtain the SB cut, as proposed in [6]. Note that the constant term $\pi_t^\top x_{t-1}$ is neglected in the Lagrangian problem as it would be subtracted in the SB cut, which is given as;

$$\theta_t \leq \sum_{m \in \mathcal{C}(t)} q_{tm} \mathcal{L}_m(\pi_m^i) + \sum_{m \in \mathcal{C}(t)} q_{tm} (\pi_m^i)^\top x_t - (p_t^i)^\top \mu_t. \tag{8a}$$

Similarly, the B cut is given as;

Preprints (www.preprints.org) | NOT PEER-REVIEWED | Posted: 13 November 2018 doi:10.20944/preprints201811.0302.v1

Peer-reviewed version available at Energies 2019, 12, 189; doi:10.3390/en12010189

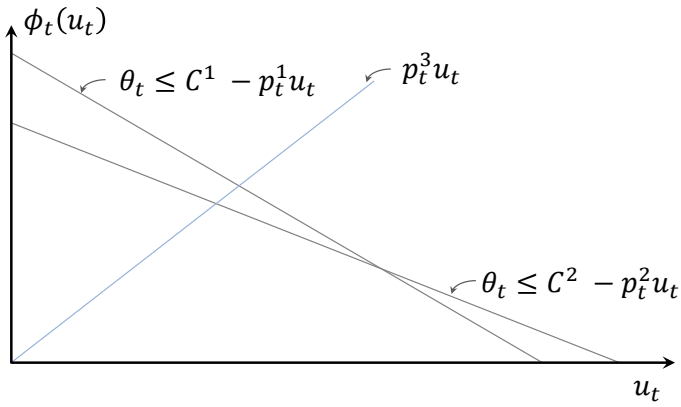

Figure 4. Illustration of the representation of the uncertain objective term price. The EFP function w.r.t. to the auxiliary variable u_t is given and x_t is assumed fixed and added to the parameter C. Observe that the cuts represent the potential for future profit, whereas the sampled objective term coefficient p_t^3 describes the present profit potential. Thus, the model can compute the trade-off between them.

$$\theta_t \leq \sum_{m \in \mathcal{C}(t)} q_{tm} \mathcal{Q}_m^{i*} + \sum_{m \in \mathcal{C}(t)} q_{tm} (\pi_m^i)^\top (x_t - x_t^*) - (p_t^i)^\top \mu_t. \tag{9a}$$

Where $\mathcal{Q}_m^{i*}$ is the objective value of BP_m^i and x_t^* is the candidate solution. The problem is solved for $m \in \mathcal{C}(t)$, where $\mathcal{C}(t)$ is the set of children nodes from a node in stage t and q_{tm} is the conditional probability. Recall that SDDP requires the stochastic variables to be stagewise independent, therefore the set $\mathcal{C}(t)$ is the same for all nodes in time stage t. The function $\phi_t^i(x_t, u_t, \tilde{\xi}_{t+1})$ is thus confined by some upper bound and the acquired set of B or SB cuts.

3.3. Uncertainty Modelling

In the following we provide some insight on how the objective term uncertainty modelling is done. For the purpose of illustration, we assume that all state variables are fixed and that we only look at the terms where the auxiliary term u_t is present. Assume that two samples of the objective term coefficient p_t^1 and p_t^2 are available, and that two cuts were constructed around these. Subsequently, a third sampling is done and the problem to be solved can be given as

$$\max_{u_t} \left\{ p_t^3 u_t + \theta_t : \theta_t \leq C_t^i - p_t^i u_t, (\theta_t, u_t) \in \mathbb{R}_+, \forall i \in \{1,2\} \right\}. \tag{10}$$

Since the state variables are assumed fixed, they are embedded in the constant term C_t^i. One can see that the problem consist of maximizing the present profit, $p_t^3 u_t$, and future profit, described by the two cuts. The problem (10) is therefore able to assert whether there is an expectancy for greater profits in the future or not, depending on the current realization of the objective term coefficient. An illustration of this is given in Figure 4.

The algorithm for how the MTHS problem is solved is given in the next section.

3.4. Solution Approach

We define Algorithm 1, based on the SDDP framework. As seen from line 14 and 16 in the algorithm, one can choose which type of cut (B or SB) to use. After a certain amount of iterations a final simulation is carried out on a larger set of scenarios.

Note that convergence cannot be guaranteed as FP_t^i is a nonconcave function w.r.t. the state variables. However, the approach will give an approximate solution that can yield good results depending on how nonconcave the *true* EFP function is. The nonconvexity of the EFP function can be

Preprints (www.preprints.org) | NOT PEER-REVIEWED | Posted: 13 November 2018 doi:10.20944/preprints201811.0302.v1

Peer-reviewed version available at *Energies* **2019**, *12*, 189; doi:10.3390/en12010189

Algorithm 1: Solving the MTHS problem

Set x_0^i, $i \leftarrow 1$, UB $= +\infty$ and LB $= -\infty$
while $i < i^{\max}$ **or some other stopping criteria do**
  Sample N scenarios $\Omega^i = \xi_1^k, \ldots, \xi_{T\,k=1,\ldots,N}^k$
  `/* Forward iteration */`
  for k=1,...,N **do**
    for t=1,...,T **do**
      Solve FP_t^i and collect solution f_t from (5)
    $\mathrm{lb}^k \leftarrow \Sigma_{t=1,\ldots,T} f_t$
  `/* Compute lower bound */`
  $\mu \leftarrow \frac{1}{N}\Sigma_{k=1}^N \mathrm{lb}^k$ and $\sigma^2 \leftarrow \frac{1}{N-1}\Sigma_{k=1}^N (\mathrm{lb}^k - \mu)^2$
  LB $\leftarrow \mu + z_\alpha \frac{\sigma}{\sqrt{N}}$
  `/* Backward iteration */`
  for t=T,..., 2 **do**
    for k=1,..., N **do**
      for $m \in \mathcal{C}(t)$ **do**
        Solve BP_t^i and collect π_m^i from (6c)
        if *B cuts* **then**
          Collect $\mathcal{Q}_t^i$ from (6)
        else if *SB cuts* **then**
          Solve LG_t^i and collect $\mathcal{L}_t^i$ from (7)
      Collect $p_t \subset r_t$ from (4)
      Add desired cut to ϕ_t^i
  `/* Compute upper bound */`
  UB $\leftarrow Q_1^i(x_0^i, u_0, \xi_0^i)$
  $i \leftarrow i + 1$
`/* Final simulation */`
Sample M scenarios $\Omega^i = \xi_1^k, \ldots, \xi_{T\,k=1,\ldots,M}^k$
for k=1,...,M **do**
  for t=1,...,T **do**
    Solve FP_t^i and collect solution f_t, x_t^{ik}, y_t^{ik} from (5)
  $\mathrm{lb}^k \leftarrow \Sigma_{t=1,\ldots,T} f_t$
`/* Compute lower bound */`
$\mu \leftarrow \frac{1}{M}\Sigma_{k=1}^M \mathrm{lb}^k$ and $\sigma^2 \leftarrow \frac{1}{M-1}\Sigma_{k=1}^M (\mathrm{lb}^k - \mu)^2$
LB $\leftarrow \mu + z_\alpha \frac{\sigma}{\sqrt{M}}$

Preprints (www.preprints.org) | NOT PEER-REVIEWED | Posted: 13 November 2018 doi:10.20944/preprints201811.0302.v1

Peer-reviewed version available at Energies 2019, 12, 189; doi:10.3390/en12010189

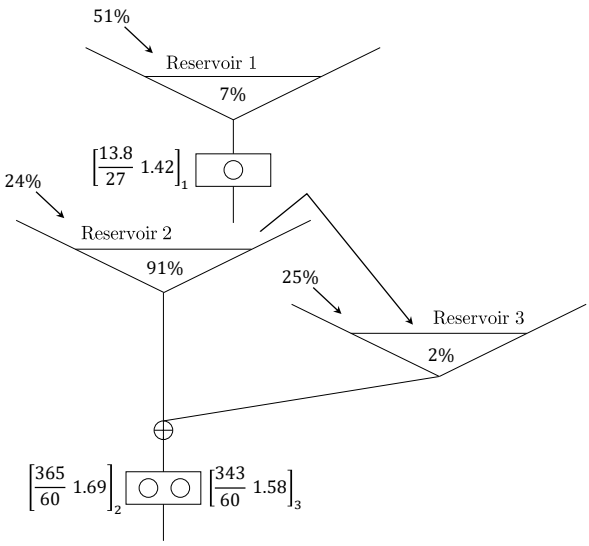

Figure 5. Illustration of the hydropower system. There are 3 reservoirs, each represented by their relative storage capacity and inflow compared to the system as a whole. As an example, reservoir no. 1 has 7% of the systems storage capacity and 51% of the inflow. The hydropower stations are represented by their maximum power at nominal head, discharge and the energy equivalent ($\frac{[\mathrm{MW}]}{[\mathrm{m}^3/\mathrm{s}]}$ $[\mathrm{MWh/m^3}]$). Since the lower power station is connected to two reservoirs it has different efficiency's, depending on what reservoir is depleted.

visualized by the approach proposed in Section 3.1. Other measures to characterize how prominent the nonconcavities are could also be performed, as in [22, Chp. 7.2.].

4. Case Study

The case study is a representation of a Norwegian hydropower system, comprising 3 reservoirs and 2 power stations. The power stations have 13.8 MW and 365 MW installed capacity. There is a short-term and long-term reservoir connected to the largest power station, as seen in Figure 5. Thus, the aim for the long-term reservoir is to store as much water for usage in the most remunerated hours during the year, while the short-term reservoirs need to be properly managed in order to avoid spillage. This system was also used as a study case in [7,23].

The VAR-1 model representing the stochastic processes was fitted to 70 historical years of inflow, and energy prices obtained from a fundamental market model generating energy prices for those 70 years [24]. Historical prices for the primary reserve market is used to describe the reserve capacity prices.

We use weekly decision stages. Each weekly decision problem consists of 1858 constraints (not considering the cuts), 1152 variables (837 continuous and 315 binary). There are 104 weeks in the scheduling horizon, and we consider 15 branches in the backward pass of the SDDP algorithm. Each week has 21 time-steps representing 3 time blocks of the day. 3 scenarios are sampled for each forward SDDP iteration, and the final simulation is carried out with 300 scenarios. We use the same sampled scenarios for all cases. From the final simulation, a confidence interval is computed. The problem was formulated in C++ with Gurobi 7.5 as the optimization solver. The computations were carried out on a computer cluster with two Intel Xeon E5-2690 v4 processors, 2.6 GHz and 384 GB RAM. No parallelization was carried out except the one from the optimization solver. Parallelization in the SDDP framework is well studied, as in [25], and thus neglected for this work. It would, however, contribute to significantly reducing the CPU time.

Preprints (www.preprints.org) | NOT PEER-REVIEWED | Posted: 13 November 2018 doi:10.20944/preprints201811.0302.v1

Peer-reviewed version available at Energies 2019, 12, 189; doi:10.3390/en12010189

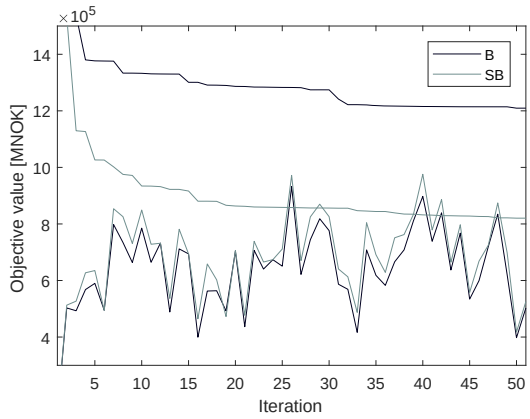

Figure 6. Convergence of the approach with Benders and Strengthened Benders cuts.

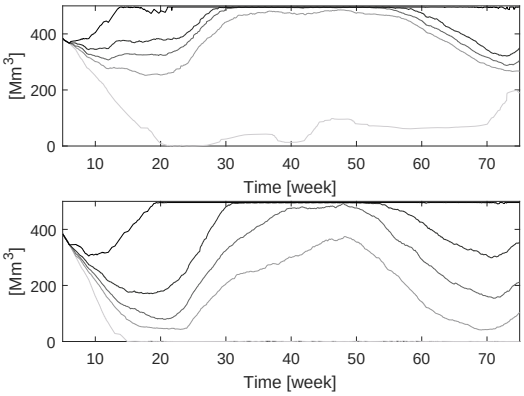

Figure 7. Percentile plot of reservoir trajectories for reservoir 2. (Top) with Benders cuts and (bottom) with Strengthened Benders cuts.

4.1. Results and Discussion

In the following, results from Algorithm 1 is outlined with use of both B and SB cuts. The MTHS problem was first solved with uncertainty of inflow, reserve capacity, and energy price. A case with only uncertainty in inflow was performed for comparison.

The convergence plot for Algorithm 1 is shown in Figure 6, when B and SB cuts where used. It is clear that the SB cuts provide significantly tighter cuts and a better policy. One can also observe that the upper bound converges slowly, and would most likely continue to improve with more iterations. The computation time does, however, become more prominent for SB cuts as seen in Table 1. Algorithm 1 required approximately 5 times longer time with SB cuts than with B cuts. The use of parallel processing could easily drive the computation time down, making the use of SB cuts better suited for daily operational use.

The expected value of water, or water values (WV), for the largest reservoir in the system are shown in Figure 8. The WVs are computed by fixing all the other state variables in the EFP function and finding the coefficients of the binding cuts. One can observe that even though the cut coefficients from both B and SB cuts come from the problem BP_t^i, the water values for the SB cuts are generally lower than the B cuts. This can be seen as a result that the right-hand-side in the SB cuts are lower, therefore, lowering the cuts which result in a lower water value for the same state, as the EFP function is concave. An illustration of this is given in Figure 9, where two cuts are generated in the first iteration of the SDDP algorithm. The coefficients of the cuts are the same for both SB and B cuts, but as seen from the top left and right plot, the SB cuts have a tighter right-hand-side. This results in the water values given in the lower plot. After consecutive iterations, the water values with SB cuts tends to stabilize on lower values, which is a reasonable observation as the SB cuts makes the model see less expected profit in the future.

A percentile plot of the reservoir trajectories for the largest reservoir is shown in Figure 7, for both B and SB cuts. The figure clearly shows how the algorithm is able to utilize the reservoir better when SB cuts are used. When B cuts are used the algorithm sees a higher expected future profit than what is achievable, resulting in a simulated operation at very high reservoir volumes. Implications of this can be seen in Figure 8a and 8c, where the change in water values is substantial around week 18, due to the spring flood giving high risk of spillage for large reservoir volumes.

In Table 1 the bounds of the algorithm are shown, computed from the final simulation, together with the percentage wise gap and computation time for the 50 forward and backward iterations. For comparison, the problem was solved with only uncertainty of inflow, that is given in the bottom half of the table. Observe how the convergence properties improve, indicating that the approach of including objective term uncertainty in SDDP by [15] requires more iterations. In validation studies using a

Preprints (www.preprints.org) | NOT PEER-REVIEWED | Posted: 13 November 2018 doi:10.20944/preprints201811.0302.v1

Peer-reviewed version available at Energies 2019, 12, 189; doi:10.3390/en12010189

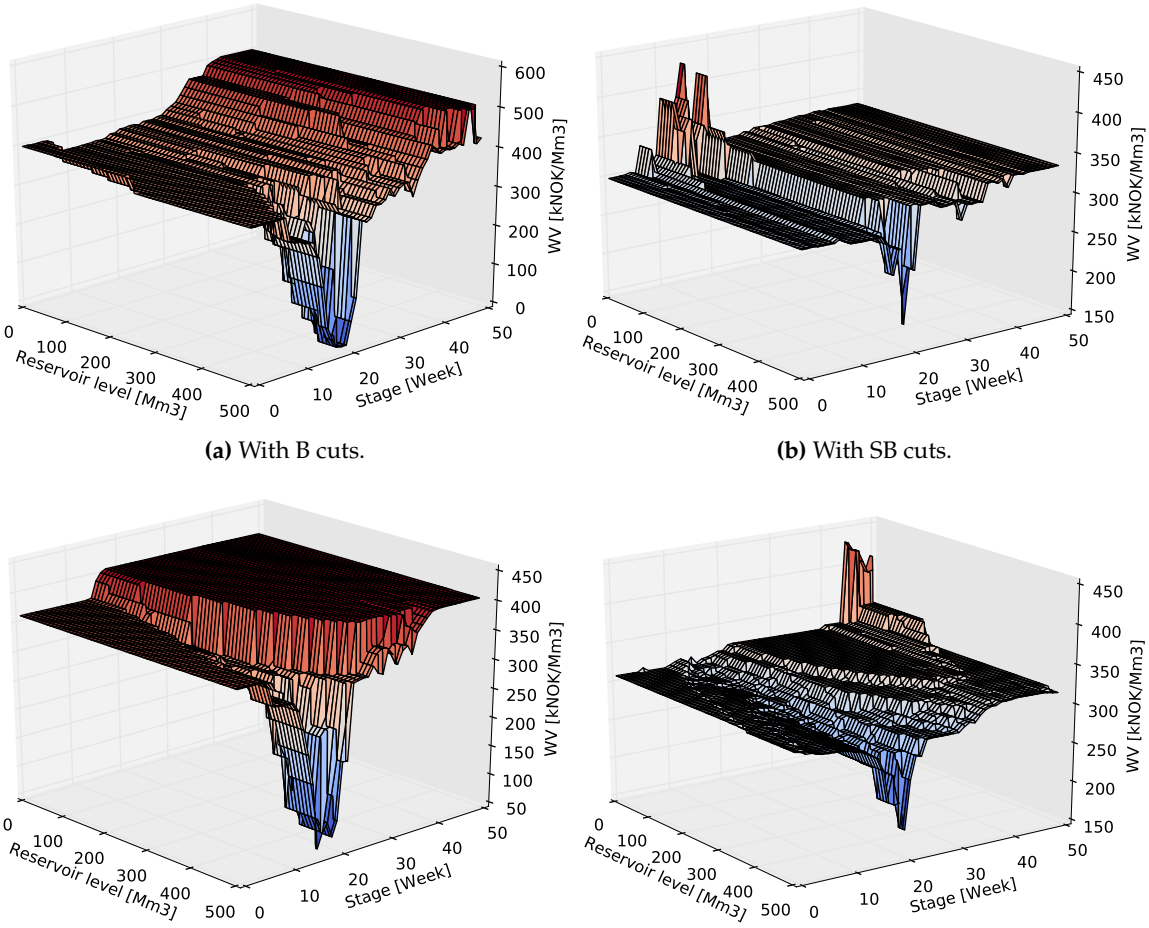

(a) With B cuts.

(b) With SB cuts.

(c) With B cuts and only uncertainty of inflow.

(d) With SB cuts and only uncertainty of Inflow.

Figure 8. Water values for reservoir 2 for the different case studies.

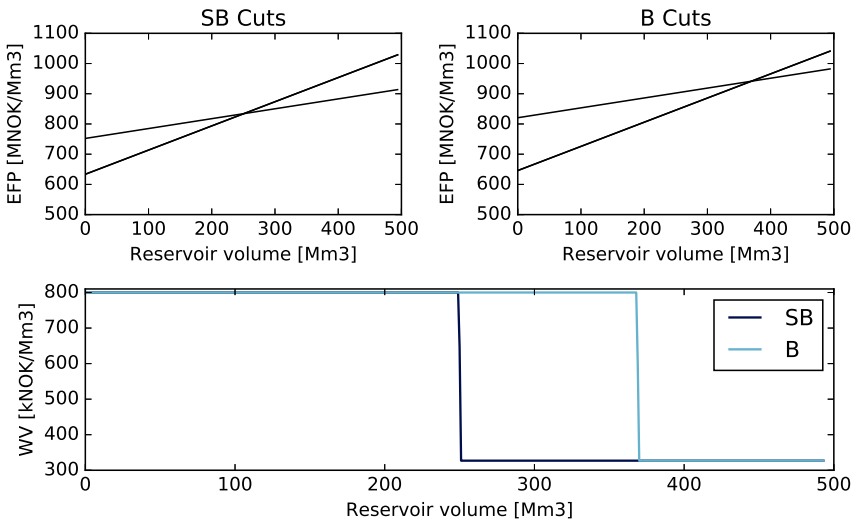

Figure 9. Illustration of the B and SB cuts and how this affects the water value.

smaller system with fewer decision stages it was observed that the approach does slowly converge.

Preprints (www.preprints.org) | NOT PEER-REVIEWED | Posted: 13 November 2018 doi:10.20944/preprints201811.0302.v1

Peer-reviewed version available at Energies 2019, 12, 189; doi:10.3390/en12010189

Table 1. Economic and computational performance of the two case studies with use of either B or SB cuts. Uncertainty of inflow, reserve capacity, and energy price (top) and uncertainty of inflow (bottom).

	UB [kNOK]	stat. LB [kNOK]	gap [%]	time [h min]
B	1 209 510	502 838	58.4	5 17
SB	820 466	525 493	36.0	23 59
B	1 017 580	537 808	47.1	5 52
SB	614 616	563 280	8.4	34 31

This illustrates the difficulty of solving multi-stage stochastic problems with high dimensions of uncertainty.

5. Conclusion

A medium-term hydropower scheduling (MTHS) problem with variable head and uncertainty in inflow, reserve capacity, and energy price was investigated. The proposed model based on the stochastic dual dynamic (SDDP) method included correlations between the different stochastic processes and allowed for representation of a detailed hydropower system.

By mean of visualization, we found that the expected future profit (EFP) function for the MTHS case study was not highly nonconcave, and we argue that the approximation of the EFP as a concave function within the SDDP method is a fair compromise between accuracy and computation time. We compared two type of Benders cuts to approximate the EFP function, namely the Benders (B) and the Strengthened Benders (SB) cuts.

In the presented case study it was found that the use of SB cuts provided a significantly better policy than with the use of B cuts. The policy improvement comes at an increased computational time, around a 5 times higher for SB than B in the case study. Moreover, we found that the inclusion of objective term uncertainty led to significantly slower convergence.

Author Contributions: Conceptualization, Martin N. Hjelmeland, Arild Helseth and Magnus Korpås; methodology, Martin N. Hjelmeland, Arild Helseth; software, Martin N. Hjelmeland; validation, Martin N. Hjelmeland, Arild Helseth and Magnus Korpås; writing—original draft preparation, Martin N. Hjelmeland; writing—review and editing, Arild Helseth and Magnus Korpås; visualization, Martin N. Hjelmeland.

Funding: This research was funded by the Research Council of Norway and industry partners under Grant 228731/E20.

Conflicts of Interest: The authors declare no conflict of interest.

Abbreviations

The following abbreviations are used in this manuscript:

B	Benders
DP	Dynamic Programming
EFP	Expected Future Profit
LP	Linear Programming
MIP	Mixed Integer Programming
MTHS	Medium-Term Hydropower Scheduling
SB	Strengthened Benders
SDDiP	Stochastic Dual Dynamic Integer Programming
SDDP	Stochastic Dual Dynamic Programming
SDP	Stochastic Dynamic Programming
WV	Water Values

Preprints (www.preprints.org) | NOT PEER-REVIEWED | Posted: 13 November 2018 doi:10.20944/preprints201811.0302.v1

Peer-reviewed version available at Energies 2019, 12, 189; doi:10.3390/en12010189

References

1. Pereira, M.V.F. Optimal Stochastic Operations Scheduling of Large Hydroelectric Systems. *International Journal of Electrical Power & Energy Systems* **1989**, *11*, 161–169. doi:Doi 10.1016/0142-0615(89)90025-2.
2. Birge, J.R. Decomposition and partitioning methods for multistage stochastic linear programs. *Operations research* **1985**, *33*, 989–1007.
3. Pereira, M.V.F.; Campodónico, N.; Kelman, R. Application of stochstic dual dp and extensions to hydrothermal scheduling. Technical Report 2, PSRI, 1999.
4. Shapiro, A.; Tekaya, W.; da Costa, J.P.; Soares, M.P. Risk neutral and risk averse stochastic dual dynamic programming method. *European Journal of Operational Research* **2013**, *224*, 375–391.
5. Gjelsvik, A.; Belsnes, M.; Haugstad, A. An algorithm for stochastic medium-term hydrothermal scheduling under spot price uncertainty. Power Systems Computation Conference (PSCC), Trondheim, Norway, 1999, 1999.
6. Zou, J.; Ahmed, S.; Sun, X.A. Stochastic dual dynamic integer programming. *Mathematical Programming* **2018**. doi:10.1007/s10107-018-1249-5.
7. Hjelmeland, M.N.; Zou, J.; Helseth, A.; Ahmed, S. Nonconvex Medium-Term Hydropower Scheduling by Stochastic Dual Dynamic Integer Programming. *IEEE Transactions on Sustainable Energy* **2018**. doi:10.1109/TSTE.2018.2805164.
8. Thome, F.; Pereira, M.V.F.; Granville, Sergio Fampa, M. Non-Convexities Representation on Hydrothermal Operation Planning using SDDP. *Working paper, 2013*.
9. Abgottspon, H.; Andersson, G. Medium-term optimization of pumped hydro storage with stochastic intrastage subproblems. Power Systems Computation Conference (PSCC)., 2014, pp. 1–7. doi:10.1109/PSCC.2014.7038352.
10. Philpott, A.B.; Wahid, F.; Bonnans, F. MIDAS: A mixed integer dynamic approximation scheme. *Optimization-online* **2016**.
11. Steeger, G.; S.Rebennack. Dynamic Convexification within Nested Benders Decomposition using Lagrangian Relaxation: An Application to the Strategic Bidding Problem. *European Journal of Operational Research* **2017**, *257*, 669–686.
12. Gjelsvik, A.; Mo, B.; Haugstad, A., Long- and Medium-term Operations Planning and Stochastic Modelling in Hydro-dominated Power Systems Based on Stochastic Dual Dynamic Programming. In *Handbook of Power Systems I*; Energy Systems, Springer Berlin Heidelberg, 2010; book section 2, pp. 33–55. doi:10.1007/978-3-642-02493-1_2.
13. Helseth, A.; Fodstad, M.; Mo, B. Optimal Medium-Term Hydropower Scheduling Considering Energy and Reserve Capacity Markets. *IEEE Transactions on Sustainable Energy* **2016**, *PP*, 1–9. doi:10.1109/TSTE.2015.2509447.
14. Baucke, R.; Downward, A.; Zakeri, G. A deterministic algorithm for solving stochastic minimax dynamic programmes. *Optimization-online* **2018**.
15. Downward, A.; Dowson, O.; Baucke, R. Stochastic dual dynamic programming with stagewise dependent objective uncertainty. *Optimization-online* **2018**.
16. Hjelmeland, M.N.; Helseth, A.; Korpås, M. Impact of Modelling Details on the Generation Function for a Norwegian Hydropower Producer. *Journal of Physics: Conference Series* **2018**, *1042*, 012010. doi:10.1088/1742-6596/1042/1/012010.
17. Fosso, O.B.; Belsnes, M.M. Short-term hydro scheduling in a liberalized power system. 2004 International Conference on Power System Technology, 2004. PowerCon 2004., 2004, Vol. 2, pp. 1321–1326 Vol.2. doi:10.1109/ICPST.2004.1460206.
18. Guedes, L.S.M.; de Mendonça Maia, P.; Lisboa, A.C.; Vieira, D.A.G.; Saldanha, R.R. A Unit Commitment Algorithm and a Compact MILP Model for Short-Term Hydro-Power Generation Scheduling. *IEEE Transactions on Power Systems* **2017**, *32*, 3381–3390. doi:10.1109/TPWRS.2016.2641390.
19. Borghetti, A.; D'Ambrosio, C.; Lodi, A.; Martello, S. An MILP Approach for Short-Term Hydro Scheduling and Unit Commitment With Head-Dependent Reservoir. *IEEE Transactions on Power Systems* **2008**, *23*, 1115–1124. doi:10.1109/TPWRS.2008.926704.

Preprints (www.preprints.org) | NOT PEER-REVIEWED | Posted: 13 November 2018 doi:10.20944/preprints201811.0302.v1

Peer-reviewed version available at *Energies* **2019**, *12*, 189; doi:10.3390/en12010189

20. Diniz, A.L.; Maceira, M.E.P. A Four-Dimensional Model of Hydro Generation for the Short-Term Hydrothermal Dispatch Problem Considering Head and Spillage Effects. *IEEE Transactions on Power Systems* **2008**, *23*, 1298–1308. doi:10.1109/TPWRS.2008.922253.
21. Cerisola, S.; Latorre, J.M.; Ramos, A. Stochastic dual dynamic programming applied to nonconvex hydrothermal models. *European journal of operational research : EJOR* **2012**, *218*, 687–697.
22. Abgottspon, H. Hydro power planning: Multi-horizon modeling and its applications. PhD thesis, ETH Zurich, 2015.
23. Hjelmeland, M.N.; Korpås, M.; Helseth, A. Combined SDDP and simulator model for hydropower scheduling with sales of capacity. 2016 13th International Conference on the European Energy Market (EEM), 2016, pp. 1–5. doi:10.1109/EEM.2016.7521187.
24. Wolfgang, O.; Haugstad, A.; Mo, B.; Gjelsvik, A.; Wangensteen, I.; Doorman, G. Hydro reservoir handling in Norway before and after deregulation. *Energy* **2009**, *34*, 1642 – 1651. 11th Conference on Process Integration, Modelling and Optimisation for Energy Saving and Pollution Reduction, doi:http://dx.doi.org/10.1016/j.energy.2009.07.025.
25. Helseth, A.; Braaten, H. Efficient Parallelization of the Stochastic Dual Dynamic Programming Algorithm Applied to Hydropower Scheduling. *Energies* **2015**, *8*, 12431. doi:10.3390/en81212431.